Received: 5 October 2023 | Revised: 24 January 2024 | Accepted: 31 January 2024

DOI: 10.1111/cas.16111

Cancer Science WILEY

ORIGINAL ARTICLE

Enhanced lipid biosynthesis in oral squamous cell carcinoma cancer-associated fibroblasts contributes to tumor progression: Role of IL8/AKT/p-ACLY axis

Pan Liu[1] | Yue Wang[1] | Xiang Li[1] | Zhenan Liu[1] | Yunqing Sun[1] | Hanzhe Liu[1] | Zhe Shao[1,2] | Erhui Jiang[1,2] | Xiaocheng Zhou[1,3] | Zhengjun Shang[1]

[1]State Key Laboratory of Oral and Maxillofacial Reconstruction and Regeneration, Key Laboratory of Oral Biomedicine Ministry of Education, Hubei Key Laboratory of Stomatology, School and Hospital of Stomatology, Wuhan University, Wuhan, China

[2]Department of Oral and Maxillofacial Head and Neck Oncology, School and Hospital of Stomatology, Wuhan University, Wuhan, China

[3]Department of Oral and Maxillofacial Surgery, School and Hospital of Stomatology, Wuhan University, Wuhan, China

Correspondence
Xiaocheng Zhou and Zhengjun Shang, The State Key Laboratory of Oral and Maxillofacial Reconstruction and Regeneration, Key Laboratory of Oral Biomedicine Ministry of Education, Hubei Key Laboratory of Stomatology, School and Hospital of Stomatology, Wuhan University, No. 237 Luoyu Road, Wuhan, Hubei Province, 430079, China.
Email: zhouxiaocheng@whu.edu.cn and shangzhengjun@whu.edu.cn

Funding information
National Natural Science Foundation of China, Grant/Award Number: 82273306 and 82203666; Natural Science Foundation of Hubei Province, Grant/Award Number: 2022CFB768

Abstract

Lipid metabolic reprogramming of tumor cells has been proven to play a critical role in tumor initiation and development. However, lipid metabolism in cancer-associated fibroblasts (CAFs) has rarely been studied, particularly in CAFs of oral squamous cell carcinoma (OSCC). Additionally, the molecular mechanism by which tumor cells regulate lipid metabolism in fibroblasts is unclear. In this study, we found that phosphorylated ATP citrate lyase (p-ACLY), a key lipid metabolic enzyme, was upregulated in OSCC CAFs. Compared to paracancerous normal fibroblasts, CAFs showed enhanced lipid synthesis, such as elevated cytosolic acetyl-CoA level and accumulation of lipid droplets. Conversely, reduction of p-ACLY level blocked this biological process. In addition, blocking lipid synthesis in CAFs or inhibiting fatty acid uptake by OSCC cells reduced the promotive effects of CAFs on OSCC cell proliferation, invasion, and migration. These findings suggested that CAFs are one of lipid sources required for OSCC progression. Mechanistically, AKT signaling activation was involved in the upregulation of p-ACLY level and lipid synthesis in CAFs. Interleukin-8 (IL8), an exocrine cytokine of OSCC cells, could activate AKT and then phosphorylate ACLY in fibroblasts. This study suggested that the IL8/AKT/p-ACLY axis could be considered as a potential target for OSCC treatment.

KEYWORDS
ATP citrate lyase, cancer-associated fibroblast, IL8, lipid metabolism, oral squamous cell carcinoma

1 | INTRODUCTION

Oral squamous cell carcinoma (OSCC) is a lethal malignancy with high recurrence and metastasis risks. Despite many efforts to combat this cancer, such as advances in diagnosis and treatment, the prognosis for patients with OSCC remains unsatisfactory, with an overall 5-year survival rate of less than 50%.[1,2] Therefore, exploring the molecular mechanisms underlying OSCC progression to discover effective therapeutic targets is in urgent need.

The tumor microenvironment (TME) is a complex dynamic system in which extensive cross-talk is established between tumor and stromal cells.[3–5] As the dominant stromal cell type in TME, cancer-associated fibroblasts (CAFs) play multiple roles in tumor progression. In addition to secreting growth factors and cytokines, remodeling the extracellular matrix (ECM), CAFs also undergo metabolic alterations and act as an energy supplier to boost tumor growth and metastasis.[6–13] Therefore, targeting CAFs as a cancer therapeutic intervention strategy has been pushed to the forefront.

Metabolic reprogramming is a hallmark of cancer. Such reprogrammed metabolism of glucose, amino acids, and lipids plays important roles in tumor initiation and development.[14–18] For instance, tumor cells largely restrict their glycometabolism to glycolysis rather than aerobic oxidation, even under oxygen-rich conditions.[15–17] With glycolysis, tumor cells can not only obtain energy at a high frequency, but also produce large amounts of lactate, creating an acidic environment that promotes tumor progression and immune evasion.[16,17] However, the perspective on cancer metabolism should not be limited to tumor cells, but should also take stromal cells into account, especially CAFs. For instance, it has been reported that CAFs from different tumor types undergo enhanced glycolysis and produce lactate for tumor cells.[11,12] Nevertheless, lipid metabolism in CAFs has been rarely studied, particularly in CAFs of OSCC.

ATP citrate lyase (ACLY) is an important metabolic enzyme that catalyzes conversion of citrate and coenzyme A to oxaloacetate and acetyl-CoA. The acetyl-CoA product is the substrate for lipid biosynthesis as well as histone acetylation.[19,20] Elevated ACLY expression or activity was detected in various cancers and associated with tumor development.[21–23] Therefore, ACLY has attracted considerable interest as a cancer therapeutic target. Nevertheless, the expression pattern and relevant role of ACLY in CAFs have not been well studied. In a recent study on melanoma,[24] our research group revealed that ACLY is enriched in extracellular vesicles of melanoma cells, especially under hypoxic conditions. Accordingly, it is reasonable to assume that tumor cells could upregulate ACLY and lipid synthesis in surrounding stromal cells, particularly CAFs. We hypothesized that OSCC cells positively regulate lipid synthesis in CAFs by increasing ACLY expression or activity, thus making CAFs one of the lipid sources for tumor cells.

In this study, we investigated the expression pattern and associated role of ACLY in OSCC CAFs. Our study revealed that elevated expression of phosphorylated ACLY (p-ACLY) in CAFs augmented lipid synthesis, making CAFs a lipid source for OSCC cells during tumor progression. In addition, interleukin-8 (IL8)-driven AKT signaling activation could promote ACLY phosphorylation and lipid synthesis in fibroblasts. This study advances our understanding of the interplay between CAFs and OSCC cells, and presents a potential therapeutic target for OSCC.

2 | MATERIALS AND METHODS

2.1 | Isolation and culture of primary fibroblasts

Fibroblast isolation was carried out as previously described.[25] Human gingival fibroblasts (HGFs) were isolated from fresh and healthy gingival tissues donated by volunteers. To isolate CAFs and paracancerous normal fibroblasts (PNFs), fresh OSCC tissues and matched paracancerous normal tissues were obtained from OSCC patients at the School and Hospital of Stomatology, Wuhan University. Fibroblasts isolated from OSCC tissues were defined as CAFs and those from paracancerous normal tissues as PNFs. The fibroblasts were cultured with DMEM containing 10% FBS at 37°C in 5% CO_2 and only used within five passages.

2.2 | Conditioned medium collection

Cells were seeded into a 6-well culture plate. When cells became a 70% confluent monolayer, they were washed twice with PBS buffer and then DMEM containing 10% or 3% dialyzed FBS (HyCyte, Suzhou, China) was added to each well. Twenty-four hours later, the medium was harvested and centrifuged at 2000 rpm for 10 min. Then the supernatant was collected and passed through a 0.22 μm filter. We used DMEM initially containing 3% dialyzed FBS to generate conditioned medium (CM) for wound healing assay; DMEM initially containing 10% dialyzed FBS was used to generate CM for CM free fatty acid (FFA) quantification, cell proliferation, and Matrigel invasion assays.

More methods are detailed in the Supplemental File S1.

3 | RESULTS

3.1 | Phosphorylated ACLY was highly expressed in OSCC CAFs

To investigate ACLY expression pattern in OSCC CAFs, we collected normal oral mucosa ($n=8$) and OSCC tissue samples ($n=46$) for immunohistochemical (IHC) staining. The results showed no significant difference in ACLY expression between normal mucosa and OSCC (Figures 1A,B-ii and S1). However, the activated form of ACLY, p-ACLY, was upregulated in OSCC tissues, including tumor cells and

FIGURE 1 Phosphorylated ATP citrate lyase (p-ACLY) was upregulated in oral squamous cell carcinoma (OSCC) cancer-associated fibroblasts (CAFs). (A) Representative immunohistochemistry images of p-ACLY, ACLY, and fibroblast activation protein (FAP) staining in normal oral mucosa and OSCC tissues. Scale bar, 100 μm. (B) Immunohistochemistry scores of p-ACLY (i), ACLY (ii), and FAP (iii) in the stromal region of normal oral mucosa and OSCC tissues. (C) p-ACLY and ACLY expression in paired paracancerous normal fibroblasts (PNFs) and CAFs was examined by western blot. (D) Quantitative analysis for western blot of (C). (i) p-ACLY expression. (ii) ACLY expression. (E) Quantitative PCR for ACLY mRNA level in paired PNFs and CAFs. Data are presented as means ± SD. Results are representative of at least three independent experiments. $^{**}p<0.01$, $^{***}p<0.001$. ns, no significance.

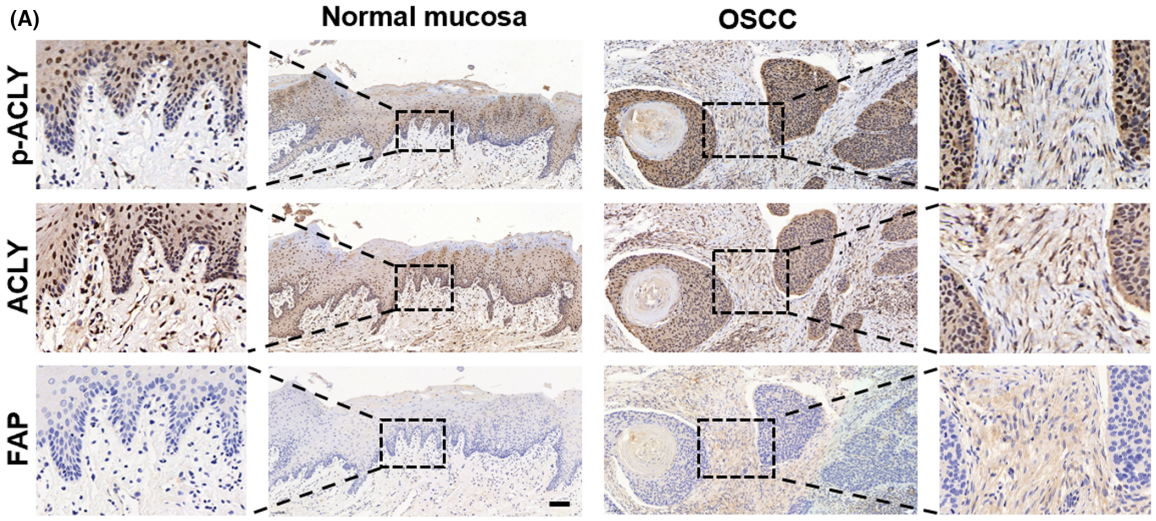
(A)
Normal mucosa
OSCC
p-ACLY
ACLY
FAP

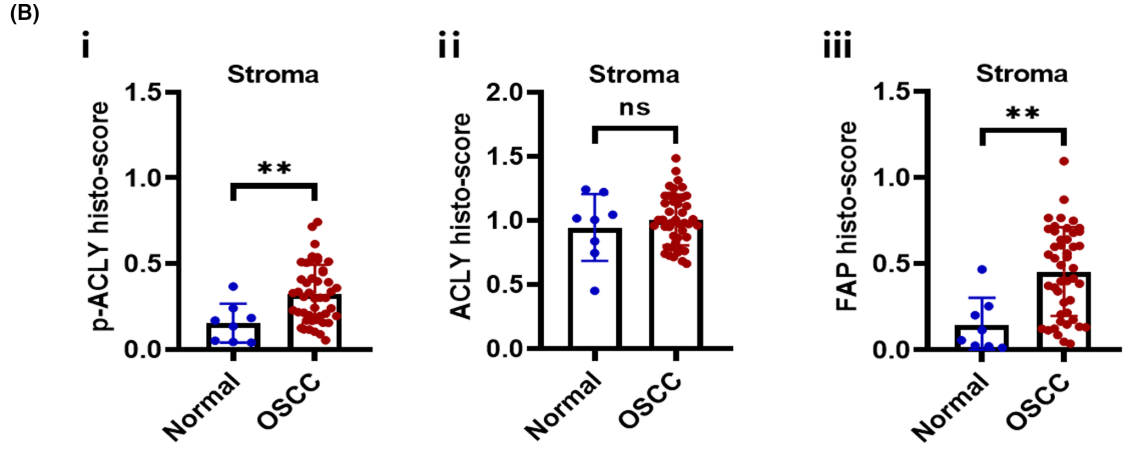
(B)
i
Stroma
p-ACLY histo-score
**
Normal
OSCC
ii
Stroma
ns
ACLY histo-score
iii
Stroma
**
FAP histo-score

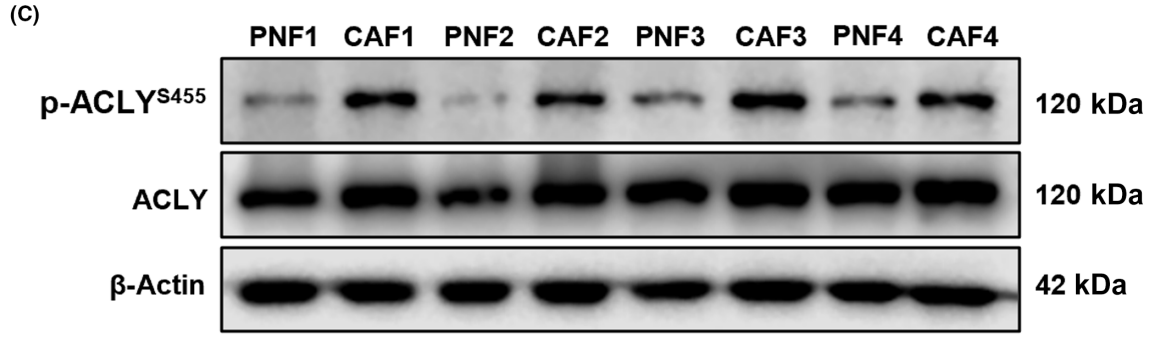
(C)
PNF1 CAF1 PNF2 CAF2 PNF3 CAF3 PNF4 CAF4
p-ACLY S455
120 kDa
ACLY
120 kDa
β-Actin
42 kDa

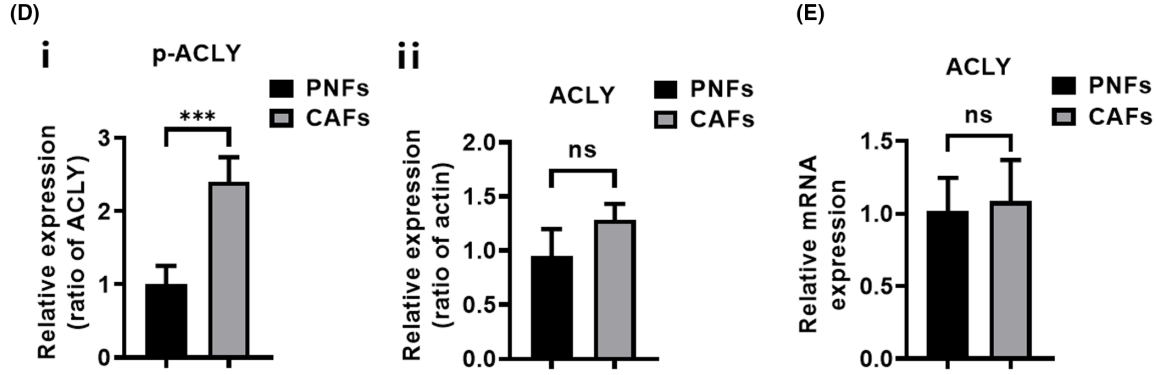
(D)
i
p-ACLY
PNFs
CAFs
***
Relative expression (ratio of ACLY)
ii
ACLY
ns
Relative expression (ratio of actin)
(E)
ACLY
ns
Relative mRNA expression

stromal cells (Figures 1A,B-i and S1). In addition, in the OSCC stromal region, p-ACLY was mainly located in fibroblast-like cells (Figure 1A), suggesting that p-ACLY expression is probably elevated in CAFs. To test this speculation, we isolated primary CAFs and PNFs, and then detected ACLY expression at mRNA and protein levels. Consistent with IHC results, quantitative PCR and western blot analysis showed no statistical difference in ACLY expression between CAFs and PNFs (Figure 1CD-ii,E). Nevertheless, it was shown by western blot analysis that CAFs had a higher p-ACLY level than PNFs (Figure 1C,D-i). Collectively, p-ACLY expression was elevated in OSCC CAFs.

3.2 | Lipid synthesis was enhanced in OSCC CAFs, whereas reduction of p-ACLY level blocked this biological process

The lipid content of PNFs and CAFs was examined by Oil red O staining. Under control conditions, the average density of lipid droplets (LDs) in CAFs was higher than that in PNFs (Figure 2A,B). Then we measured the level of acetyl-CoA, the substrate for lipid synthesis, in the cytosol of these cells. The acetyl-CoA measurement assay showed that CAFs had a higher cytosolic acetyl-CoA level than PNFs (Figure 2C). Moreover, we quantified FFA, a lipid metabolite, in the CM of PNFs and CAFs. The FFA quantification assay revealed that the concentration of FFA in CAF CM is higher than that in PNF CM (Figure 2D). These results suggested that OSCC CAFs underwent enhanced lipid synthesis.

To verify the role of p-ACLY in regulating lipid synthesis of CAFs, we treated CAFs with ACLY inhibitor NDI-091143. Western blot analysis revealed that this inhibitor reduced the p-ACLY level of CAFs in time- and dose-dependent manners (Figure 2E). After NDI-091143 treatment (40 μM for 24 h), the cytosolic acetyl-CoA level in CAFs decreased significantly (Figure 2C). In addition, CAFs under NDI-091143 treatment showed reduced intracellular LD density and CM FFA concentration (Figure 2A,B,D). Furthermore, the Gene Ontology enrichment analysis revealed that treatment with NDI-091143 downregulated the lipid biosynthetic process in CAFs significantly (Figure 2F). Overall, p-ACLY upregulated lipid synthesis in CAFs.

3.3 | Blocking lipid synthesis in CAFs or inhibiting fatty acid uptake by OSCC cells reduced the tumor-promoting effects of CAFs

Given enhanced lipid synthesis in OSCC CAFs, we speculated that CAFs could promote tumor progression through the lipid metabolic pathway. To verify this speculation, we collected CM from OSCC cells, PNFs, CAFs, and CAFs pretreated with NDI-091143. Then OSCC cell lines including CAL27 and SCC25 were treated with each CM. The CCK-8 proliferation, Matrigel invasion, and wound healing assays revealed that OSCC cells treated with CAF CM showed enhanced proliferation, invasion, and migration abilities, compared to those treated with PNF CM or OSCC cell CM (Figures 3A–C and S2). However, this trend was attenuated when CAFs were pretreated with NDI-091143 (Figures 3A–C and S2). These results suggested that reduction of p-ACLY level reduced tumor-promoting effects of CAFs, which was likely to result from lipid synthesis blockade.

CD36 has been reported to be the best characterized membrane fatty acid translocase mediating the uptake of fatty acids.[26–28] CD36 expression and plasma membrane localization are sensitive to the concentration of exogenous fatty acids, and are critical for its function in promoting fatty acid uptake.[29,30] To further determine whether CAFs could promote tumor progression through the lipid metabolic pathway, we detected CD36 expression in OSCC cells cultured with indicated CM. It was shown that CAF CM elevated total and membrane expression of CD36 in OSCC cells, whereas pretreatment of CAFs with NDI-091143 reversed this process (Figures 3D and S3). These results suggested that lipid metabolites released from CAFs were taken up by OSCC cells. Then we treated OSCC cells with CD36 inhibitor sulfosuccinimidyl oleate sodium (SSO) before treating them with CAF CM. The results showed that SSO pretreatment (50 μM, 12 h) also reduced the promotive effects of CAFs on OSCC cell proliferation, invasion, and migration (Figures 3E–G and S4). Taken together, lipid metabolites released from CAFs could be taken up by OSCC cells and contribute to OSCC progression.

3.4 | AKT signaling activation involved in upregulation of lipid synthesis in CAFs

AKT signaling has been reported as one of the pathways regulating ACLY phosphorylation.[18] Thus, we detected the phosphorylated AKT (p-AKT) level in paired PNFs and CAFs. Western blot analysis showed that the level of p-AKT in CAFs was significantly higher than that in PNFs (Figure 4A). We then treated CAFs with AKT inhibitor MK2206 (10 μM, 12 h) and examined p-ACLY levels by western blot analysis. It was shown that CAFs under MK2206 treatment showed a dramatic decrease in both p-AKT and p-ACLY levels (Figure 4B). In addition, the intracellular LD density, cytosolic acetyl-CoA level, and CM FFA concentration of CAFs were significantly reduced by MK2206 treatment (Figure 4C–F). Moreover, treatment with MK2206 reduced the promotive effects of CAFs on

FIGURE 2 Oral squamous cell carcinoma (OSCC) cancer-associated fibroblasts (CAFs) underwent enhanced lipid synthesis, whereas reduction of phosphorylated ATP citrate lyase (p-ACLY) level blocked this biological process. (A) Intracellular lipid droplets (LDs) were visualized by Oil red O staining. Scale bar, 10 μm. (B) Quantitative analysis for intracellular LDs of (A). (C) Cytosolic acetyl-CoA measurement was carried out on paracancerous normal fibroblasts (PNFs), CAFs, and CAFs treated with NDI-091143 (NDI; 40 μM, 24 h). (D) Relative free fatty acid (FFA) level in conditioned medium (CM) from PNFs, CAFs, and CAFs pretreated with NDI-091143. (E) p-ACLY level in CAFs under NDI-091143 treatment was detected by western blot. (i) Concentration gradient. (ii) Time gradient. (F) (i) Differentially expressed genes identified by RNA sequencing. (ii) Bubble plots of Gene Ontology enrichment analysis related to CAFs under NDI-091143 treatment. Data are presented as means ± SD. Results are representative of at least three independent experiments. $^{*}p < 0.05$, $^{**}p < 0.01$. ns, no significance.

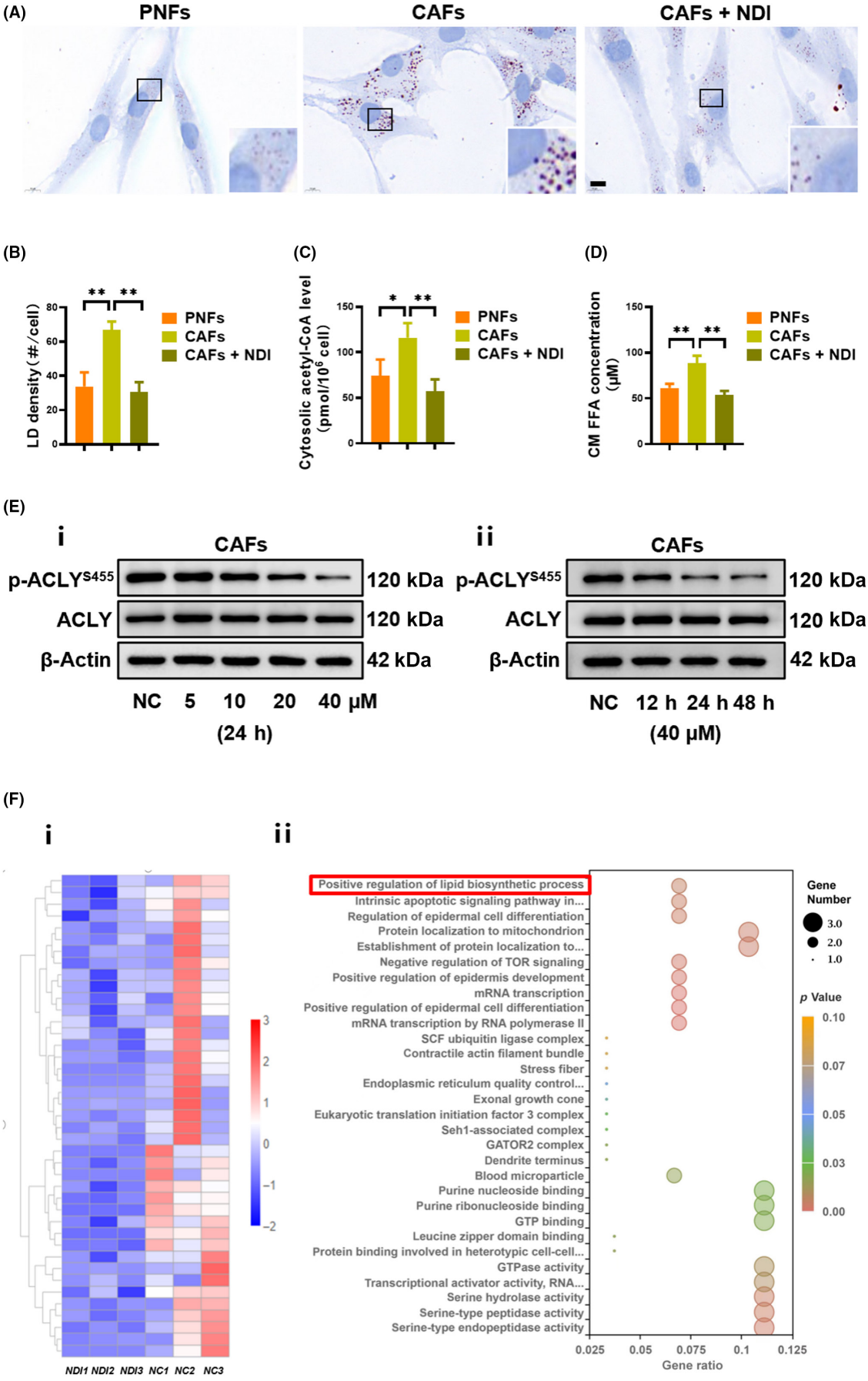
(A)
PNFs
CAFs
CAFs + NDI
(B)
LD density (#/cell)
PNFs
CAFs
CAFs + NDI
(C)
Cytosolic acetyl-CoA level (pmol/10^6 cell)
PNFs
CAFs
CAFs + NDI
(D)
CM FFA concentration (μM)
PNFs
CAFs
CAFs + NDI
(E)
i
CAFs
p-ACLY S455
ACLY
β-Actin
120 kDa
120 kDa
42 kDa
NC 5 10 20 40 μM
(24 h)
ii
CAFs
p-ACLY S455
ACLY
β-Actin
120 kDa
120 kDa
42 kDa
NC 12 h 24 h 48 h
(40 μM)
(F)
i
NDI1 NDI2 NDI3 NC1 NC2 NC3
ii
Positive regulation of lipid biosynthetic process
Intrinsic apoptotic signaling pathway in...
Regulation of epidermal cell differentiation
Protein localization to mitochondrion
Establishment of protein localization to...
Negative regulation of TOR signaling
Positive regulation of epidermis development
mRNA transcription
Positive regulation of epidermal cell differentiation
mRNA transcription by RNA polymerase II
SCF ubiquitin ligase complex
Contractile actin filament bundle
Stress fiber
Endoplasmic reticulum quality control...
Exonal growth cone
Eukaryotic translation initiation factor 3 complex
Seh1-associated complex
GATOR2 complex
Dendrite terminus
Blood microparticle
Purine nucleoside binding
Purine ribonucleoside binding
GTP binding
Leucine zipper domain binding
Protein binding involved in heterotypic cell-cell...
GTPase activity
Transcriptional activator activity, RNA...
Serine hydrolase activity
Serine-type peptidase activity
Serine-type endopeptidase activity
Gene ratio
Gene Number
p Value

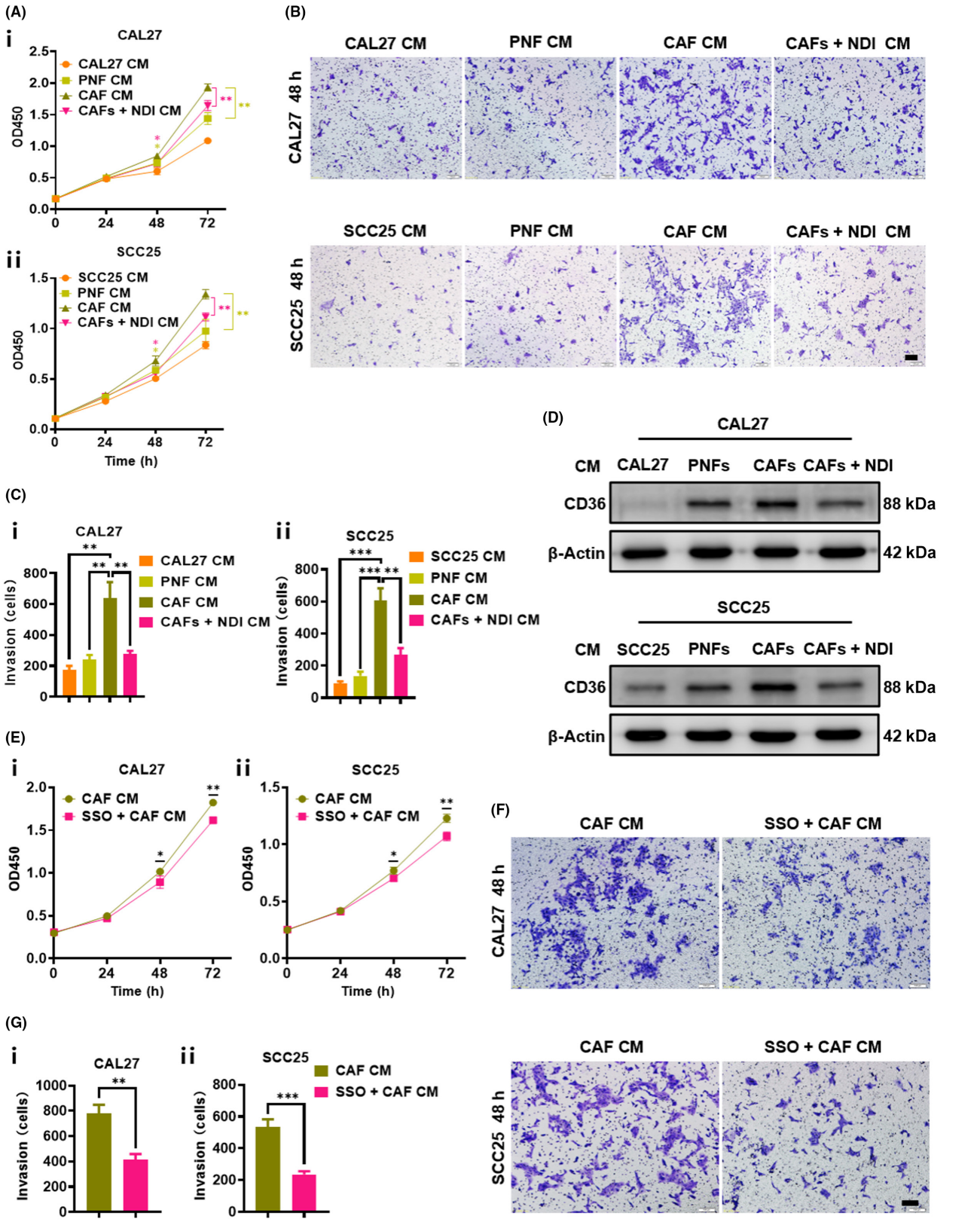

FIGURE 3 Blocking lipid synthesis in cancer-associated fibroblasts (CAFs) or inhibiting fatty acid uptake by oral squamous cell carcinoma (OSCC) cells reduced the tumor-promoting effects of CAFs. (A, E) Cell proliferation rates of OSCC cells treated with indicated conditioned medium (CM) were examined by CCK-8 proliferation assay. (i) CAL27, (ii) SCC25. (B, F) Cell invasion abilities of OSCC cells treated with indicated CM were examined by Matrigel invasion assay. Scale bar, 100 μm. (C, G) Quantitative analysis for invasion cells of (B, F). (i) CAL27, (ii) SCC25. (D) CD36 expression of OSCC cells treated with indicated CM was detected by western blot analysis. Data are presented as means ± SD. Results are representative of at least three independent experiments. $^{**}p < 0.01$, $^{***}p < 0.001$. NDI, NDI-091143; ns, no significance; OD450, optical density at 450 nm; PNF, paracancerous normal fibroblast; SSO, sulfosuccinimidyl oleate sodium.

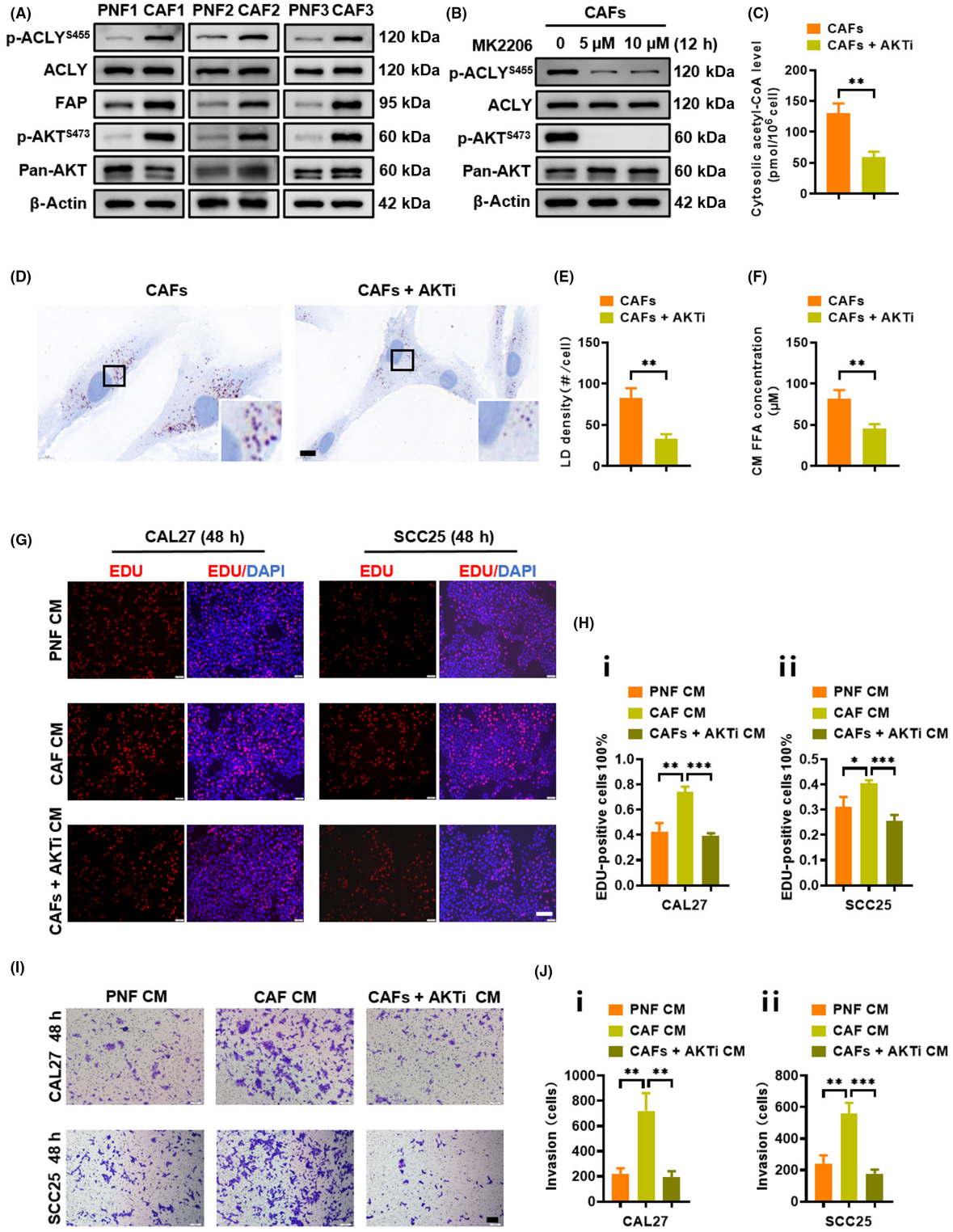

FIGURE 4 AKT signaling activation was involved in the upregulation of lipid synthesis in cancer-associated fibroblasts (CAFs). (A) Expression of phosphorylated ATP citrate lyase (p-ACLY), ACLY, p-AKT, AKT, and fibroblast activation protein (FAP) in paired paracancerous normal fibroblasts (PNFs) and CAFs was detected by western blot analysis. (B) Expression of p-ACLY, ACLY, p-AKT and AKT in MK2206-treated CAFs was detected by western blot analysis. (C) Measurement of cytosolic acetyl-CoA in MK2206-treated CAFs. (D) Intracellular lipid droplets (LDs) in MK2206-treated CAFs were visualized by Oil red O staining. Scale bar, 10 μm. (E) Quantitative analysis for intracellular LDs of (D). (F) Relative free fatty acid (FFA) levels in the conditioned medium (CM) of MK2206-treated CAFs. (G) Cell proliferation rates of oral squamous cell carcinoma (OSCC) cells treated with indicated CM were examined by EdU proliferation assay. Scale bar, 100 μm. (H) Quantitative analysis for EdU-positive cells of (G). (i) CAL27, (ii) SCC25. (I) Cell invasion abilities of OSCC cells treated with indicated CM were examined by Matrigel invasion assay. Scale bar, 100 μm. (J) Quantitative analysis for invasion cells of (I). (i) CAL27, (ii) SCC25. Data are presented as means ± SD. Results are representative of at least three independent experiments. $^{*}p < 0.05$, $^{**}p < 0.01$, $^{***}p < 0.001$.

OSCC cell proliferation, invasion, and migration (Figures 4G–J and S5). Together, AKT signaling activation was involved in the upregulation of lipid synthesis in CAFs.

3.5 | Interleukin-8 triggered ACLY phosphorylation and lipid synthesis in fibroblasts through AKT signaling activation

To elucidate the mechanism by which OSCC cells regulate p-ACLY level and lipid synthesis in fibroblasts, we searched for exocrine molecules of OSCC cells that can function as AKT agonists. Interleukin-8 (IL8) was identified in previously published reports as a possible upstream regulator.[31–35] We examined IL8 expression in The Cancer Genome Atlas database using the GEPIA website. Results indicated that IL8 was upregulated in head and neck squamous cell carcinoma tissues (Figure 5A). To examine IL8 expression in OSCC, we collected OSCC tissue samples ($n=46$) and normal oral mucosa ($n=8$) for IHC staining. Results showed that IL8 was highly expressed in OSCC tissues (Figure 5B,C). In addition, we detected IL8 expression in OSCC cells and Human immortalized oral epithelial cells (HIOECs) by western blot analysis. The results revealed that OSCC cells had a higher IL8 protein level than HIOECs (Figure 5D). Moreover, we quantified IL8 levels in the CM of OSCC cells and HIOECs. The IL8 ELISA showed that the concentration of IL8 in OSCC cell CM was significantly higher than that in HIOEC CM (Figure 5E). These results indicated that IL8 was an exocrine cytokine of OSCC cells.

To investigate whether IL8 could upregulate p-ACLY level and lipid synthesis in fibroblasts, we used HGFs as the research candidate. Then HGFs were treated with exogenous IL8 at different concentrations. Western blot analysis showed that IL8 (50 ng/mL) upregulated p-ACLY level in HGFs significantly (Figure 5F). Plus, HGFs treated with IL8 (50 ng/mL, 24 h) showed an increase in cytosolic acetyl-CoA level (Figure 5G), CM FFA concentration (Figure 5H), and intracellular LD density (Figure 5I,J). These results suggested that IL8 could elevate p-ACLY level and lipid synthesis in fibroblasts.

To determine whether AKT signaling participates in IL8-mediated upregulation of lipid synthesis in HGFs, we detected p-AKT and p-ACLY levels in IL8-treated HGFs. Western blot analysis showed that the p-AKT level in IL8-treated HGFs gradually increased from 0 min to 60 min and then decreased over time, which was consistent with the change of p-ACLY level (Figure 5K). Then we treated HGFs with MK2206 (10 μM, 12 h) prior to IL8 stimulation. Results showed that IL8-mediated elevations of p-ACLY level and lipid synthesis in HGFs was blocked by MK2206 pretreatment (Figure 5G–J,L). These results indicated that IL8 upregulated p-ACLY level and lipid synthesis in HGFs through AKT signaling activation.

3.6 | Inhibition of p-ACLY or combined with AKT inhibitor suppressed OSCC growth in vivo

To reduce the effect of drug nontargeting on experimental results, we used CAL27, which has the lowest p-ACLY expression among several OSCC cell lines, to establish xenograft tumors (Figure S6A). The mice from indicated groups were treated with NDI-091143 and/or MK2206. As expected, treatments with NDI-091143 and/or MK2206 suppressed tumor formation ability in mice (Figures 6A and S6B). Tumor growth curves and tumor weight showed NDI-091143 or MK2206 treatment slowed down tumor growth, with the combination treatment group having the smallest tumor volume and lowest tumor weight (Figure 6B,C). Moreover, IHC results revealed that stromal p-ACLY expression in xenograft tumors decreased in mice treated with NDI-091143 and/or MK2206, with the lowest p-ACLY expression in the combination treatment group (Figure 6D,E). However, there was no statistical difference in p-ACLY expression between NDI-091143 treatment group and MK2206 treatment group (Figure 6E). Additionally, we found that NDI-091143 treatment had no apparent effect on tumor growth in the CAL27 alone injection group (Figure S7), indicating that p-ACLY inhibition could reduce the promotive effect of CAFs on OSCC progression in vivo. Collectively, the results indicated that inhibition of p-ACLY or combined with AKT inhibitor suppressed OSCC progression in vivo.

4 | DISCUSSION

In TME, dynamic and multifaceted interaction between tumor and stromal cells creates favorable conditions for tumor development. As the dominant stromal cell type, CAFs interact with tumor cells through cell-to-cell contact, secreting molecules, and remodeling ECM, thereby promoting tumor progression and stimulating therapy resistance.[3,5] Investigating the cross-talk between CAFs and tumor

FIGURE 5 Interleukin-8 (IL8) triggered ATP citrate lyase (ACLY) phosphorylation and lipid synthesis in fibroblasts through AKT signaling activation. (A) IL8 expression in head and neck squamous cell carcinoma (HNSC) from The Cancer Genome Atlas database. (B) Representative immunohistochemistry (IHC) images of IL8 staining in normal oral mucosa and oral squamous cell carcinoma (OSCC) tissues. Scale bar, 100 μm. (C) IHC score of IL8 in normal oral mucosa and OSCC tissues. (D) Western blot analysis was carried out to detect IL8 expression in Human immortalized oral epithelial cells (HIOECs) and OSCC cells. (E) Quantitative analysis of IL8 level in the conditioned medium (CM) of HIOECs and OSCC cells. (F) p-ACLY and ACLY expression in human gingival fibroblasts (HGFs) stimulated by IL8 was examined by western blot. (G) Cytosolic acetyl-CoA measurement was carried out on HGFs with indicated treatments. (H) Relative free fatty acid (FFA) levels in the CM of HGFs with indicated treatments. (I) Intracellular lipid droplets (LDs) of HGFs with indicated treatments were visualized by Oil red O staining. Scale bar, 10 μm. (J) Quantitative analysis for intracellular LDs of (I). (K, L) p-ACLY, ACLY, p-AKT, and AKT expression in HGFs with indicated treatments was examined by western blot. Data are presented as means ± SD. Results are representative of at least three independent experiments $^{*}p<0.05$, $^{**}p<0.01$, $^{***}p<0.001$.

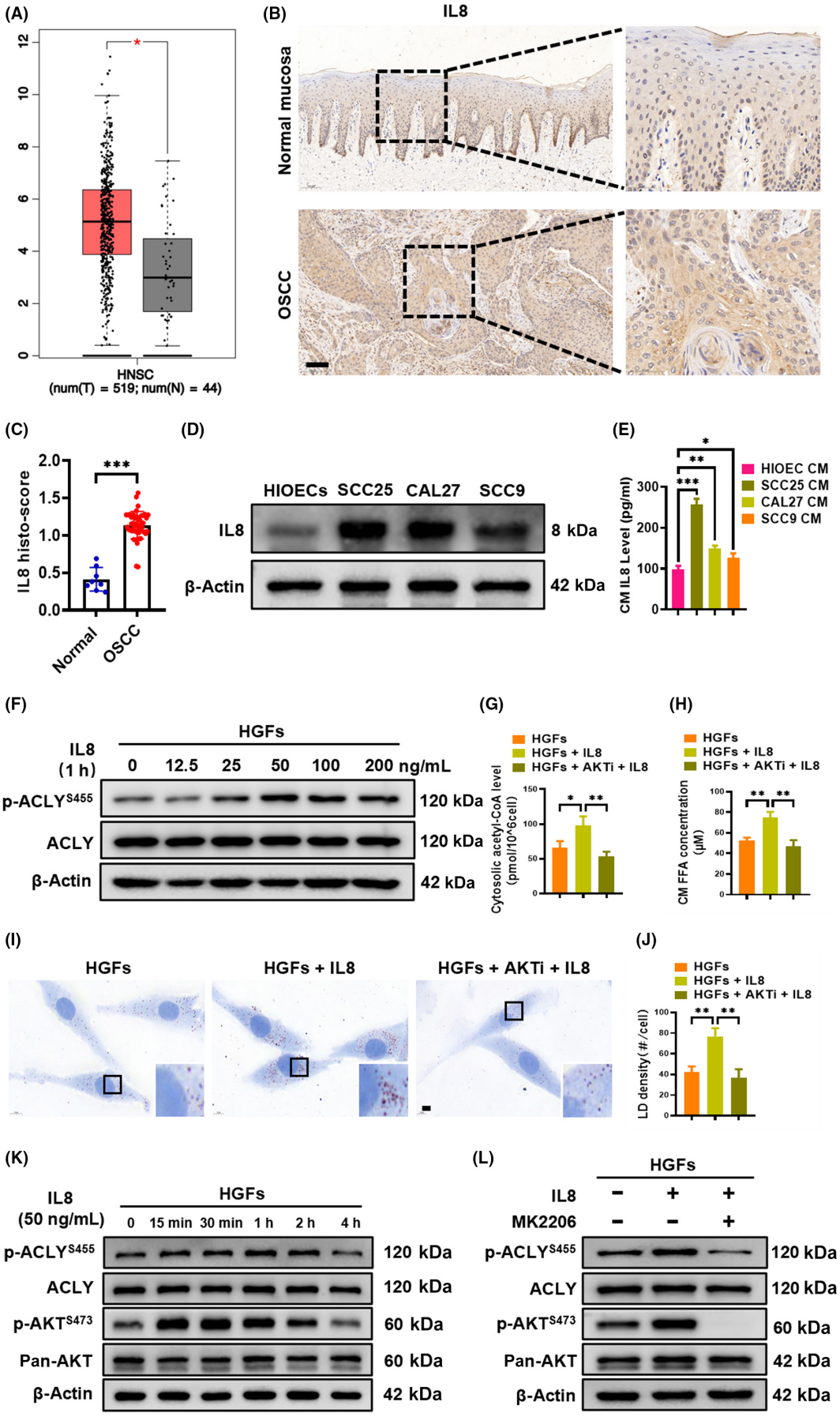
(A)
HNSC
(num(T) = 519; num(N) = 44)
(B)
IL8
Normal mucosa
OSCC
(C)
IL8 histo-score
Normal
OSCC
(D)
HIOECs SCC25 CAL27 SCC9
IL8
8 kDa
β-Actin
42 kDa
(E)
CM IL8 Level (pg/ml)
HIOEC CM
SCC25 CM
CAL27 CM
SCC9 CM
(F)
HGFs
IL8 (1 h)
0 12.5 25 50 100 200 ng/mL
p-ACLY S455
ACLY
β-Actin
120 kDa
120 kDa
42 kDa
(G)
HGFs
HGFs + IL8
HGFs + AKTi + IL8
Cytosolic acetyl-CoA level (pmol/10^6cell)
(H)
CM FFA concentration (μM)
(I)
HGFs
HGFs + IL8
HGFs + AKTi + IL8
(J)
LD density (#/cell)
(K)
IL8 (50 ng/mL)
HGFs
0 15 min 30 min 1 h 2 h 4 h
p-ACLY S455
ACLY
p-AKT S473
Pan-AKT
β-Actin
120 kDa
120 kDa
60 kDa
60 kDa
42 kDa
(L)
HGFs
IL8
MK2206
p-ACLY S455
ACLY
p-AKT S473
Pan-AKT
β-Actin
120 kDa
120 kDa
60 kDa
42 kDa
42 kDa

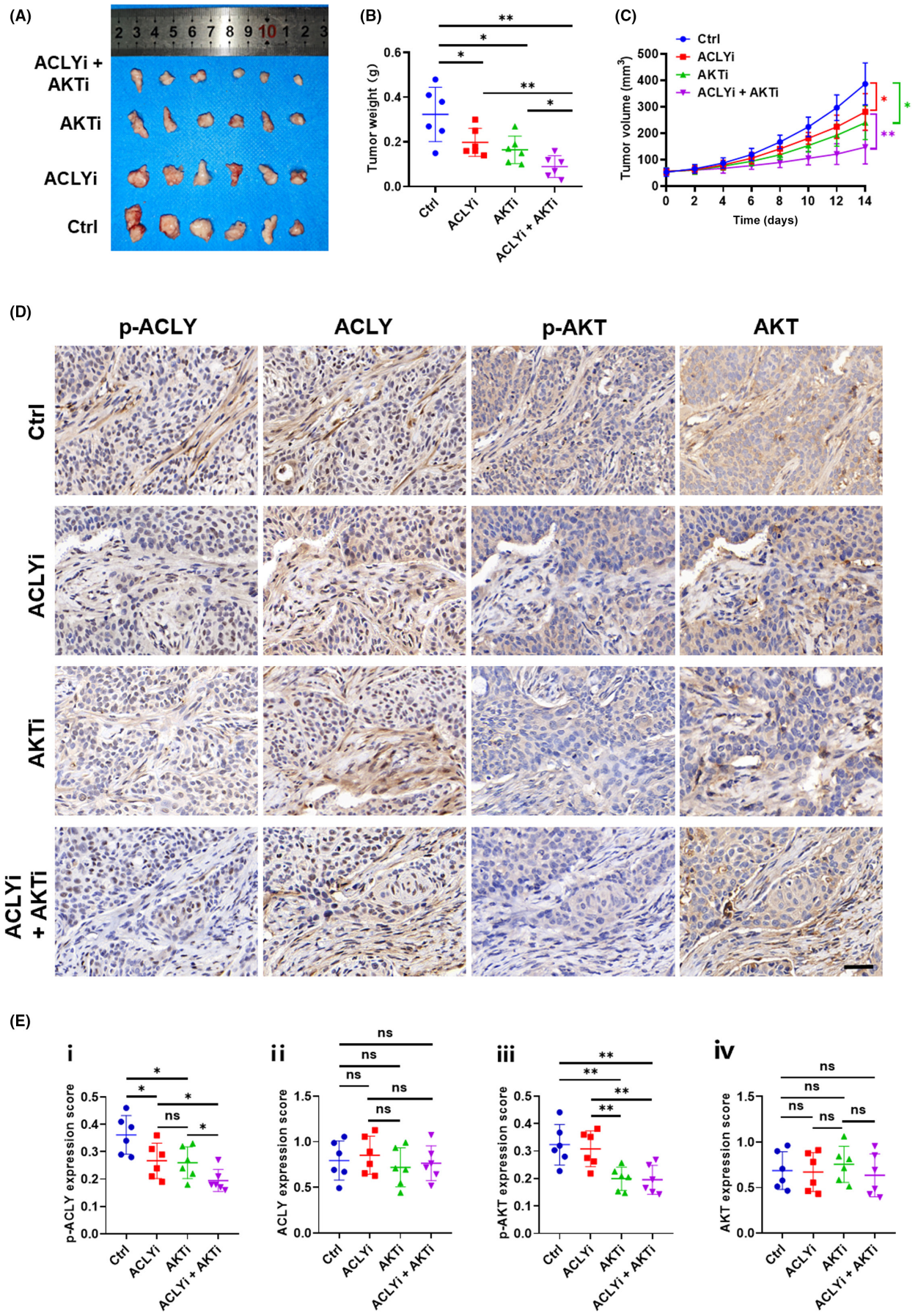
(A)
ACLYi + AKTi
AKTi
ACLYi
Ctrl
(B)
Tumor weight (g)
Ctrl
ACLYi
AKTi
ACLYi + AKTi
(C)
Ctrl
ACLYi
AKTi
ACLYi + AKTi
Tumor volume (mm3)
Time (days)
(D)
p-ACLY
ACLY
p-AKT
AKT
Ctrl
ACLYi
AKTi
ACLYi + AKTi
(E)
i
p-ACLY expression score
ii
ACLY expression score
iii
p-AKT expression score
iv
AKT expression score

FIGURE 6 Inhibition of phosphorylated ATP citrate lyase (p-ACLY) or combined with AKT inhibitor suppressed oral squamous cell carcinoma growth in vivo. (A) Images of xenograft tumors excised from nude mice. (B) Weights of xenograft tumors excised from nude mice after indicated treatments. (C) The volume of xenograft tumors was measured every 2 days after indicated treatments. (D) Expression of p-ACLY, ACLY, p-AKT, and AKT in xenograft tumors was examined by immunohistochemistry (IHC). Scale bar, 50 μm. (E) IHC scores of p-ACLY (i), ACLY (ii), p-AKT (iii), and AKT (iv) in the stromal region of xenograft tumors. Data are presented as means ± SD. Results are representative of at least three independent experiments. $^{*}p < 0.05$, $^{**}p < 0.01$. Ctrl, control; ns, no significance.

FIGURE 7 Pathway illustration of the interleukin-8 (IL8)/AKT/ phosphorylated ATP citrate lyase (p-ACLY) axis promoting oral squamous cell carcinoma (OSCC) progression. OSCC-derived IL8 activates AKT signaling in fibroblasts followed by intracellular phosphorylation of ACLY, leading to enhanced lipid synthesis. Lipid metabolites are then released from fibroblasts and taken up by OSCC cells through CD36. Absorption of exogenous lipids contributes to the invasion, proliferation, and migration of OSCC cells.

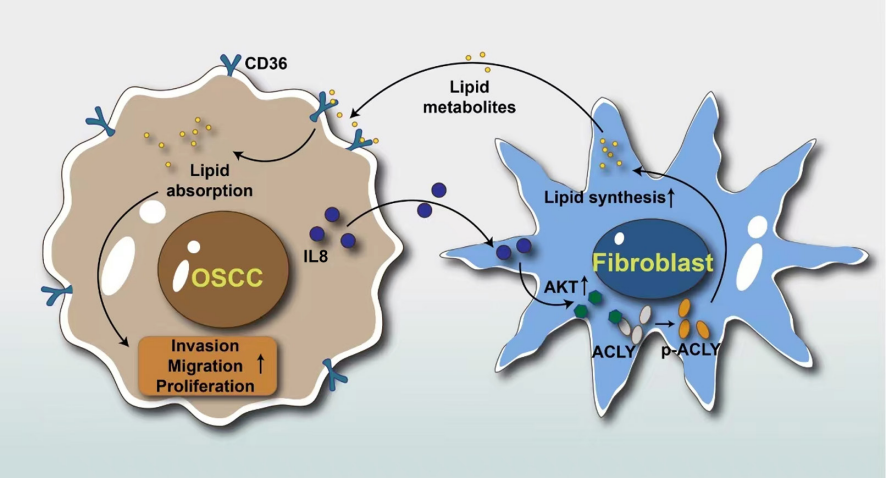

cells is of great significance for the discovery of effective cancer therapeutic targets. In present study, we found that p-ACLY was highly expressed in OSCC CAFs and it mediated the lipid metabolic interaction between CAFs and OSCC cells to facilitate tumor progression. Furthermore, we uncovered a novel mechanism by which tumor cells regulate lipid synthesis in fibroblasts. Interleukin-8, an exocrine cytokine of OSCC cells, could trigger ACLY phosphorylation and lipid synthesis in fibroblasts through AKT signaling activation. Thus, the IL8/AKT/p-ACLY axis (Figure 7) could be considered as a potential therapeutic target for OSCC.

Lipid metabolic reprogramming is one of the most remarkable metabolic alterations in cancer.[18] Tumor cells use adaptive changes in lipid metabolism, such as de novo lipogenesis and enhanced uptake of exogenous lipids, in order to form biofilms, obtain energy by fatty acid oxidation, and generate lipid mediators as signaling molecules, thus meeting their needs for rapid proliferation and metastasis.[18,36,37] Although lipid metabolism in tumor cells has been extensively studied over the past decades, much less is known about the lipid metabolic profile of stromal cells, particularly CAFs. Recent studies have shown that CAFs are one of lipid sources for tumor cells. For instance, in colorectal cancer, CAFs underwent lipid metabolic reprogramming and lipid metabolites from CAFs promoted cancer metastasis.[10] In lung adenocarcinoma, CAF-derived oleic acids could enhance the stemness of tumor cells.[38] Thus, it can be seen that lipid metabolic alteration in CAFs also plays an important role in tumor development. To date, however, there have been no reports on lipid metabolism of OSCC CAFs. In our research, we found that p-ACLY was significantly upregulated in OSCC CAFs, and CAFs showed elevated cytosolic acetyl-CoA level, intracellular LD density and CM FFA concentration, indicating enhanced lipid synthesis. In addition, CAF CM increased total and membrane expression of CD36 in OSCC cells while blocking lipid synthesis in CAFs reversed this process, suggesting that lipid metabolites released from CAFs were taken up by OSCC cells. Furthermore, blocking lipid synthesis in CAFs or inhibiting CD36 in tumor cells reduced the promotive effects of CAFs on OSCC cell proliferation, invasion, and migration. These results suggested that CAFs could promote OSCC progression through lipid metabolic pathway, which was consistent with previous studies.

Interleukin-8, a Glu-Leu-Arg (ELR+) family chemokine, was initially found to chemoattract neutrophils in inflammatory diseases by binding to its receptors CXCR1/2.[39,40] It has now been shown that IL8 is not only an inflammatory chemokine, but also a procancer factor. Substantial elevation of IL8 expression was detected in various types of cancer including OSCC, and IL8 has been reported to stimulate angiogenesis, recruit immunosuppressive cells, promote epithelial-to-mesenchymal transition, and enhance stemness and chemoresistance of tumor cells.[39–42] Notably, activation of AKT signaling is one of the major mechanisms by which IL8 regulates the phenotype and function of tumor and stromal cells. Du et al.[34] reported that the IL8/CXCR1/AKT axis enhanced anoikic resistance and metastasis of osteosarcoma cells. Huang et al.[35] showed that the IL8/AKT/HK2/PD-L1 axis induced immunosuppression in gastric cancer. However, so far, the IL8/AKT axis in modulating TME lipid metabolism has not been reported. As ACLY could be phosphorylated by AKT signaling,[18] we hypothesized that the IL8/AKT/p-ACLY axis is involved in the upregulation of lipid synthesis in fibroblasts. In our research, we found that the level of p-AKT in CAFs was higher than that in PNFs. When AKT signaling was blocked, both ACLY phosphorylation level and LD density in CAFs were significantly reduced, which suggested that AKT signaling activation was involved in the upregulation of lipid synthesis in CAFs. On the other hand, we found that IL8 was highly expressed in OSCC tissues and OSCC

cell lines, as well as in the CM of OSCC cells, indicating that IL8 was an exocrine molecule of OSCC cells. In addition, HGFs under IL8 treatment showed elevated levels of p-AKT, p-ACLY, and LD density, whereas pretreatment with AKT inhibitor blocked these elevations. Our results suggested that the IL8/AKT/p-ACLY axis was involved in the upregulation of fibroblast lipid synthesis by OSCC cells.

The current study also has some limitations. First, lipidomic analysis was not undertaken to determine the specific lipid type released by CAFs that potentiates OSCC development. Second, the relationship between lipid metabolism and the phenotype of OSCC CAFs was not investigated. Recent studies have shown that dysregulated lipid metabolism, such as accumulated LDs, is critical for the function and phenotype maintenance of CAFs in other cancer types.[43,44] In view of these aspects, further work needs to be done to investigate the lipid metabolic pathways based on our findings, aiming at suppressing OSCC progression.

In conclusion, this study determined that OSCC CAFs could promote tumor progression through the lipid metabolic pathway, which could be driven by tumor cells through paracrine cytokines. This reciprocal interplay between CAFs and tumor cells provides a new perspective on OSCC progression and is helpful in identifying new therapeutic targets for OSCC.

AUTHOR CONTRIBUTIONS

Pan Liu: Data curation; formal analysis; investigation; writing – original draft. **Yue Wang:** Investigation. **Xiang Li:** Investigation. **Zhenan Liu:** Methodology. **Yunqing Sun:** Investigation. **Hanzhe Liu:** Investigation. **Zhe Shao:** Resources. **Erhui Jiang:** Resources. **Xiaocheng Zhou:** Funding acquisition; supervision. **Zhengjun Shang:** Supervision; writing – review and editing.

ACKNOWLEDGMENTS

The authors would like to acknowledge the technical support from Xinyue Luo (Wuhan University). Pan liu and Yue Wang contributed equally to this work.

FUNDING INFORMATION

National Natural Science Foundation of China (Nos. 82273306 and 82203666) and Hubei Provincial Natural Science Foundation (No. 2022CFB768).

CONFLICT OF INTEREST STATEMENT

The authors declare no conflict of interest.

ETHICS STATEMENTS

Approval of the research protocol by an institutional review board: The study protocol was approved by the School and Hospital of Stomatology, Wuhan University.

Informed consent: Informed consent was obtained from all subjects for tissue sample collection.

Registry and the registration no. of the study: Ethics Committee of School and Hospital of Stomatology, Wuhan University, 2022-A41.

Animal studies: All procedures involving animal experiments were authorized by the Ethics Committee of Wuhan University Center for Animal Experiment. Grant number: WP20230116.

ORCID

Zhe Shao https://orcid.org/0000-0003-2357-3760
Zhengjun Shang https://orcid.org/0000-0002-4884-8129

REFERENCES

1. Eckert AW, Wickenhauser C, Salins PC, Kappler M, Bukur J, Seliger B. Clinical relevance of the tumor microenvironment and immune escape of oral squamous cell carcinoma. *J Transl Med*. 2016;14:85.
2. Zini A, Czerninski R, Sgan-Cohen HD. Oral cancer over four decades: epidemiology, trends, histology, and survival by anatomical sites. *J Oral Pathol Med*. 2010;39(4):299-305.
3. Jiang E, Yan T, Xu Z, Shang Z. Tumor microenvironment and cell fusion. *Biomed Res Int*. 2019;2019:5013592.
4. Hinshaw DC, Shevde LA. The tumor microenvironment innately modulates cancer progression. *Cancer Res*. 2019;79(18):4557-4566.
5. Elhanani O, Ben-Uri R, Keren L. Spatial profiling technologies illuminate the tumor microenvironment. *Cancer Cell*. 2023;41(3):404-420.
6. Ganguly D, Chandra R, Karalis J, et al. Cancer-associated fibroblasts: versatile players in the tumor microenvironment. *Cancers (Basel)*. 2020;12(9):2652.
7. Dou D, Ren X, Han M, et al. Cancer-associated fibroblasts-derived exosomes suppress immune cell function in breast cancer via the miR-92/PD-L1 pathway. *Front Immunol*. 2020;11:2026.
8. Tang X, Hou Y, Yang G, et al. Stromal miR-200s contribute to breast cancer cell invasion through CAF activation and ECM remodeling. *Cell Death Differ*. 2016;23(1):132-145.
9. Zhang H, Deng T, Liu R, et al. CAF secreted miR-522 suppresses ferroptosis and promotes acquired chemo-resistance in gastric cancer. *Mol Cancer*. 2020;19(1):43.
10. Zhang C, Wang XY, Zhang P, et al. Cancer-derived exosomal HSPC111 promotes colorectal cancer liver metastasis by reprogramming lipid metabolism in cancer-associated fibroblasts. *Cell Death Dis*. 2022;13(1):57.
11. Jiang E, Xu Z, Wang M, et al. Tumoral microvesicle-activated glycometabolic reprogramming in fibroblasts promotes the progression of oral squamous cell carcinoma. *FASEB J*. 2019;33(4):5690-5703.
12. Sung JS, Kang CW, Kang S, et al. ITGB4-mediated metabolic reprogramming of cancer-associated fibroblasts. *Oncogene*. 2020;39(3):664-676.
13. Xia L, Oyang L, Lin J, et al. The cancer metabolic reprogramming and immune response. *Mol Cancer*. 2021;20(1):28.
14. Sivanand S, Vander Heiden MG. Emerging roles for branched-chain amino acid metabolism in cancer. *Cancer Cell*. 2020;37(2):147-156.
15. Danhier P, Bański P, Payen VL, et al. Cancer metabolism in space and time: beyond the Warburg effect. *Biochim Biophys Acta Bioenerg*. 2017;1858(8):556-572.
16. Ippolito L, Sonveaux P, Chiarugi P. Unconventional roles of lactate along the tumor and immune landscape. *Trends Endocrinol Metab*. 2022;33(4):231-235.
17. Pérez-Tomás R, Pérez-Guillén I. Lactate in the tumor microenvironment: an essential molecule in cancer progression and treatment. *Cancers (Basel)*. 2020;12(11):3244.
18. Snaebjornsson MT, Janaki-Raman S, Schulze A. Greasing the wheels of the cancer machine: the role of lipid metabolism in cancer. *Cell Metab*. 2020;31(1):62-76.
19. Wei J, Leit S, Kuai J, et al. An allosteric mechanism for potent inhibition of human ATP-citrate lyase. *Nature*. 2019;568(7753):566-570.

20. Icard P, Wu Z, Fournel L, Coquerel A, Lincet H, Alifano M. ATP citrate lyase: a central metabolic enzyme in cancer. *Cancer Lett*. 2020;471:125-134.
21. Wen J, Min X, Shen M, et al. ACLY facilitates colon cancer cell metastasis by CTNNB1. *J Exp Clin Cancer Res*. 2019;38(1):401.
22. Wei X, Shi J, Lin Q, et al. Targeting ACLY attenuates tumor growth and acquired cisplatin resistance in ovarian cancer by inhibiting the PI3K-AKT pathway and activating the AMPK-ROS pathway. *Front Oncol*. 2021;11:642229.
23. Adorno-Cruz V, Hoffmann AD, Liu X, et al. ITGA2 promotes expression of ACLY and CCND1 in enhancing breast cancer stemness and metastasis. *Genes Dis*. 2020;8(4):493-508.
24. Tang H, Zhou X, Zhao X, et al. HSP90/IKK-rich small extracellular vesicles activate pro-angiogenic melanoma-associated fibroblasts via the NF-κB/CXCL1 axis. *Cancer Sci*. 2022;113(4):1168-1181.
25. Li X, Jiang E, Zhao H, et al. Glycometabolic reprogramming-mediated proangiogenic phenotype enhancement of cancer-associated fibroblasts in oral squamous cell carcinoma: role of PGC-1α/PFKFB3 axis. *Br J Cancer*. 2022;127(3):449-461.
26. Yang P, Qin H, Li Y, et al. CD36-mediated metabolic crosstalk between tumor cells and macrophages affects liver metastasis. *Nat Commun*. 2022;13(1):5782.
27. Ko CW, Qu J, Black DD, Tso P. Regulation of intestinal lipid metabolism: current concepts and relevance to disease. *Nat Rev Gastroenterol Hepatol*. 2020;17(3):169-183.
28. Nickerson JG, Alkhateeb H, Benton CR, et al. Greater transport efficiencies of the membrane fatty acid transporters FAT/CD36 and FATP4 compared with FABPpm and FATP1 and differential effects on fatty acid esterification and oxidation in rat skeletal muscle. *J Biol Chem*. 2009;284(24):16522-16530.
29. Yang P, Su C, Luo X, et al. Dietary oleic acid-induced CD36 promotes cervical cancer cell growth and metastasis via up-regulation Src/ERK pathway. *Cancer Lett*. 2018;438:76-85.
30. Wang J, Hao JW, Wang X, et al. DHHC4 and DHHC5 facilitate fatty acid uptake by Palmitoylating and targeting CD36 to the plasma membrane. *Cell Rep*. 2019;26(1):209-221.e5.
31. Hwang YS, Lee SK, Park KK, Chung WY. Secretion of IL-6 and IL-8 from lysophosphatidic acid-stimulated oral squamous cell carcinoma promotes osteoclastogenesis and bone resorption. *Oral Oncol*. 2012;48(1):40-48.
32. Joshi S, Pandey R, Kumar A, Gupta V, Arya N. Targeted blockade of interleukin-8 negates metastasis and chemoresistance via Akt/Erk-NFκB axis in oral cancer. *Cytokine*. 2023;166:156155.
33. Lopez-Labady J, Bologna-Molina R, Villarroel-Dorrego M. Expression of interleukin-1ß and Interleukin-8 in Oral potentially malignant disorders and carcinomas. *Front Oral Health*. 2021;2:649406.
34. Du L, Han XG, Tu B, et al. CXCR1/Akt signaling activation induced by mesenchymal stem cell-derived IL-8 promotes osteosarcoma cell anoikis resistance and pulmonary metastasis. *Cell Death Dis*. 2018;9(7):714.
35. Huang C, Chen B, Wang X, et al. Gastric cancer mesenchymal stem cells via the CXCR2/HK2/PD-L1 pathway mediate immunosuppression. *Gastric Cancer*. 2023;26(5):691-707.
36. Cheng C, Geng F, Cheng X, Guo D. Lipid metabolism reprogramming and its potential targets in cancer. *Cancer Commun (Lond)*. 2018;38(1):27.
37. Yi M, Li J, Chen S, et al. Emerging role of lipid metabolism alterations in cancer stem cells. *J Exp Clin Cancer Res*. 2018;37(1):118.
38. Hwang SH, Yang Y, Jung JH, Kim Y. Oleic acid from cancer-associated fibroblast promotes cancer cell stemness by stearoyl-CoA desaturase under glucose-deficient condition. *Cancer Cell Int*. 2022;22(1):404.
39. Han ZJ, Li YB, Yang LX, Cheng HJ, Liu X, Chen H. Roles of the CXCL8-CXCR1/2 Axis in the tumor microenvironment and immunotherapy. *Molecules*. 2021;27(1):137.
40. Teijeira A, Garasa S, Ochoa MC, et al. IL8, neutrophils, and NETs in a collusion against cancer immunity and immunotherapy. *Clin Cancer Res*. 2021;27(9):2383-2393.
41. Pu Y, Li Q, Wang Y, et al. pERK-mediated IL8 secretion can enhance the migration, invasion, and cisplatin resistance of CD10-positive oral cancer cells. *BMC Cancer*. 2021;21(1):1283.
42. Yang F, Liu XQ, He JZ, et al. Occludin facilitates tumour angiogenesis in bladder cancer by regulating IL8/STAT3 through STAT4. *J Cell Mol Med*. 2022;26(8):2363-2376.
43. Nardi F, Fitchev P, Franco OE, et al. PEDF regulates plasticity of a novel lipid-MTOC axis in prostate cancer-associated fibroblasts. *J Cell Sci*. 2018;131(13):jcs213579.
44. Zhang Y, Gu Z, Wan J, et al. Stearoyl-CoA desaturase-1 dependent lipid droplets accumulation in cancer-associated fibroblasts facilitates the progression of lung cancer. *Int J Biol Sci*. 2022;18(16):6114-6128.

SUPPORTING INFORMATION

Additional supporting information can be found online in the Supporting Information section at the end of this article.

How to cite this article: Liu P, Wang Y, Li X, et al. Enhanced lipid biosynthesis in oral squamous cell carcinoma cancer-associated fibroblasts contributes to tumor progression: Role of IL8/AKT/p-ACLY axis. *Cancer Sci*. 2024;115:1433-1445. doi:10.1111/cas.16111